

# Structured Progressive Knowledge Activation for LLM-Driven Neural Architecture Search

Zhen Liu<sup>\*1,4</sup> Yuhan Liu<sup>\*2</sup> Jinjun Wang<sup>1</sup> Wei Song<sup>3</sup> Jianyi Liu<sup>1</sup> Jingwen Fu<sup>4</sup>

## Abstract

This paper focuses on a key challenge in Neural Architecture Search (NAS): integrating established architectural knowledge while exploring new designs under expensive evaluations. Large language models (LLMs) are a promising assistant for NAS because they can translate rich architectural and coding priors into executable code edits. However, in practice, seemingly local revisions often propagate into non-local behavioral and performance shifts because a single edit can inadvertently couple multiple interacting functional factors, a phenomenon we refer to as functional entanglement. To make LLM knowledge usable under such entanglement, we propose Structured Progressive Knowledge Activation (SPARK), which activates relevant priors by explicitly selecting the functional factor to modify and conditioning the edit on that factor. This factor-conditioned editing reduces entangled side effects and yields more targeted, reliable architecture modifications. On CLRS-DFS, SPARK achieves a  $28.1\times$  sample-efficient architecture evolution speedup and yields a 22.9% relative improvement in OOD accuracy.

## 1. Introduction

This paper studies a central tension in Neural Architecture Search (NAS): integrating established architectural knowledge while exploring new designs under expensive evaluations. This tension is exacerbated by the enormous search space of neural architectures and the high cost of training and evaluation, which makes naive exploration impractical (Zoph & Le, 2017b; Real et al., 2017; Liu et al., 2019).

<sup>\*</sup>Equal contribution <sup>1</sup>State Key Laboratory of Human-Machine Hybrid Augmented Intelligence, Institute of Artificial Intelligence and Robotics, Xi’an Jiaotong University. <sup>2</sup>MiLM Plus, Xiaomi Inc. <sup>3</sup>North China University of Technology, Beijing. <sup>4</sup>Zhongguancun Academy, Beijing, China. Correspondence to: Jingwen Fu <fu-jingwen@bza.edu.cn>.

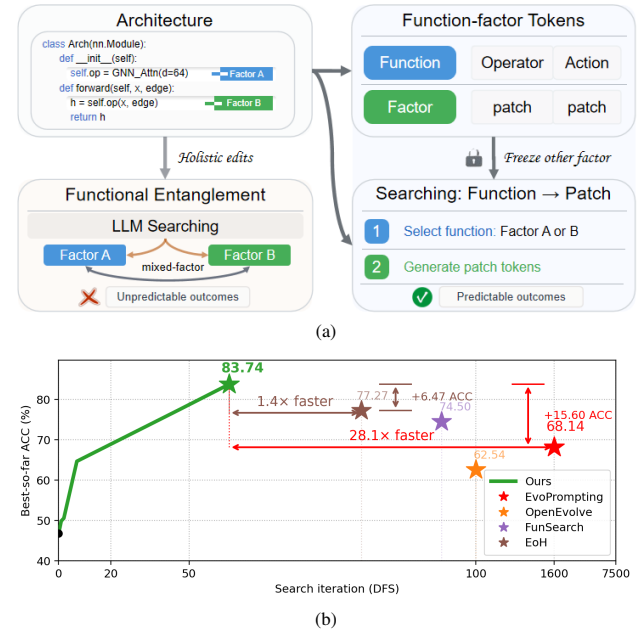


Figure 1. Motivation for structure-guided editing in LLM-driven NAS. (a) Free-form edits entangle functional factors and often break interfaces, while factor-scoped tokens enable where-to-how edits to isolate the intervention target. (b) CLRS-DFS results show faster progress and higher OOD accuracy with fewer search iterations.

LLM-driven NAS is a promising direction because it brings this balance into executable code space: a language model can propose or revise architecture programs by drawing on rich coding and architectural priors, while feedback from training and evaluation guides subsequent iterations (Chen et al., 2023). Yet, in practice, these priors often fail to translate into reliable and controllable edits, becoming a key bottleneck for effective search.

A primary reason is that architecture programs encode multiple interacting functional decisions whose dependencies are largely implicit in code. As illustrated in Fig. 1a (left), “Holistic edits” in free-form “LLM Searching” often update “Factor A” and “Factor B” together (a “mixed-factor” revision); we call this failure mode functional entanglement. In our setting, “Factor A” corresponds to the Operator factor (which computation module is used), and “Factor B” corre-

sponds to the Action factor (how the operator is invoked and wired under interface and shape constraints). Both factors are functional because together they specify the executable computation graph that determines model behavior. When a single revision entangles these factors, even seemingly local code changes can propagate into non-local behavior and performance shifts and can also break executability (e.g., by violating interface or shape consistency), yielding “Unpredictable outcomes.”

These observations suggest that the bottleneck in LLM-driven NAS is not the absence of architectural knowledge, but the lack of a mechanism that turns LLM priors into controllable edits under functional entanglement. To make priors actionable, revisions should be factor-isolated under functional entanglement, matching the constraint in Fig. 1a (right) (“Freeze other factor”). We therefore introduce “Function-factor Tokens” that expose functional factors as explicit, selectable choices, instantiated as Operator and Action, each paired with a dedicated patch slot for localized code changes. This representation supports the structured editing primitive “Searching: Function→Patch”: first “Select function: Factor A or B” (i.e., select Operator or Action), then “Generate patch tokens” to realize an executable update conditioned on the selected factor, which promotes more “Predictable outcomes” by isolating the edited factor.

Guided by this principle, we propose Structured Progressive Knowledge Activation (SPARK), a structure-guided editing operator for LLM-driven NAS. SPARK turns free-form rewriting into “Searching: Function→Patch” by decomposing each revision into the two explicit steps in Fig. 1a: “Select function: Factor A or B” and “Generate patch tokens,” while enforcing “Freeze other factor” through factor-conditioned patching. By making the intervention factor explicit and restricting each step to one factor at a time, SPARK reduces cross-factor interference between Operator and Action, mitigates entangled side effects, and improves the executability and reliability of generated candidates.

We evaluate SPARK on the CLRS algorithmic reasoning benchmark (Veličković et al., 2022), which instantiates NAS as program-structured architecture tasks under a standardized training and evaluation protocol. On CLRS-DFS, SPARK achieves a  $28.1\times$  sample-efficient architecture evolution speedup and improves OOD accuracy from 68.14% to 83.74% (a +15.6-point gain) (Fig. 1b). Across 10 CLRS tasks, SPARK achieves 83.92% mean OOD accuracy with essentially unchanged compute relative to the CLRS reference. Beyond aggregate accuracy, we study search dynamics and reliability by tracking best-so-far progress and executability, relating improvements to fewer invalid proposals and reduced Operator–Action interference.

**Contributions.** (1) We identify functional entanglement as a systematic failure mode of “Holistic edits” in free-form “LLM Searching”: single revisions become “mixed-factor” (“Factor A” and “Factor B” jointly updated), leading to “Unpredictable outcomes” including non-local behavior/performance shifts and frequent executability violations. (2) We introduce SPARK, which implements factor-isolated editing via factor selection and factor-conditioned patch generation, operationalized as “Searching: Function→Patch” with “Function-factor Tokens” (“Select function: Factor A or B,” “Generate patch tokens,” and “Freeze other factor”). (3) On CLRS program-structured architecture tasks, SPARK achieves 83.74% OOD accuracy on DFS with 57 evaluated candidates, yielding a  $28.1\times$  sample-efficient architecture evolution speedup over EvoPrompting; it further attains 83.92% mean OOD accuracy across 10 tasks with essentially unchanged compute, and we analyze search dynamics via best-so-far progress and executability.

## 2. Related Work

**NAS.** Neural architecture search (NAS) automates model design by exploring an architecture space under a validation objective. Representative paradigms include reinforcement-learning controllers (Zoph & Le, 2017a), evolutionary search with explicit variation operators (Real et al., 2019), and continuous relaxations for differentiable search (Liu et al., 2019). To reduce evaluation cost, one-shot and weight-sharing methods amortize training by reusing super-net weights (Pham et al., 2018), while standardized benchmarks improve reproducibility and fair comparison (Dong & Yang, 2020). A common practice in these pipelines is to specify a structure-aware search operator (e.g., mutate a particular edge/operator, perturb a cell, or update a relaxed parameterization), which makes the effects of each step easier to control and attribute. This property becomes fragile in LLM-driven NAS, where the search step is implemented as free-form code rewriting rather than an explicit operator, making functional roles implicit and edits harder to control.

**LLM-driven NAS.** Recent work explores LLMs for code-level NAS as architecture generators/refiners and as adaptive mutation operators under evaluation feedback (Chen et al., 2023; Zheng et al., 2023; Nasir et al., 2024; Wu et al., 2023). Beyond direct edits, LLM priors have also been leveraged via distilled design principles for warm-starting (Zhou et al., 2025), by coupling reflection with zero-cost proxies (Ji et al., 2025), and by coordinating multiple LLM roles during search (Li et al., 2025b). These methods demonstrate that LLM priors can guide exploration, but the per-iteration update is often treated as a single holistic rewrite or proposal. As a result, interacting functional decisions that are not explicitly surfaced in code can be coupled within one revision, such as changing an operator together with its

action-level wiring and related interface/shape constraints. In our setting, this holistic-edit regime can induce Functional Entanglement, where Operator and Action factors are jointly modified, making the effect of an edit harder to attribute and reducing how precisely architectural priors are activated and reused across rounds.

### Iterative LLM optimization and structured editing.

A parallel literature studies iterative refinement loops that improve outputs using self-feedback or external signals (Madaan et al., 2023; Shinn et al., 2023; Yang et al., 2024; Fernando et al., 2024). LLMs have also been integrated with evolutionary computation and program search as mutation/crossover operators and proposal mechanisms (Lehman et al., 2022; Meyerson & Miikkulainen, 2023; Šurina et al., 2025; Hemberg & O’Reilly, 2024), with surveys systematizing this emerging interplay (Wu et al., 2025b). Separately, structure-aware code generation/editing constrains outputs to grammars or ASTs (Yin & Neubig, 2017; Rabinovich et al., 2017), and program repair restores compilability/executability from erroneous code (Gupta et al., 2017). These lines motivate validity constraints, but they do not directly address the NAS-specific failure mode we study: multi-round evolution in architecture code where implicit functional roles allow a single free-form edit to couple Operator-level changes with Action-level wiring, leading to Functional Entanglement. Our work complements them by making Operator/Action factors explicit via Function-factor Tokens and enforcing factor-isolated edits at the iteration level through Searching: Function→Patch, together with feasibility checks, to reduce cross-factor interference in LLM-driven NAS.

## 3. Method

### 3.1. Problem Setup

We study LLM-driven multi-round neural architecture search (NAS) in code space (Chen et al., 2023), where each candidate architecture is represented as executable code  $a \in \mathcal{A}$  implementing a neural algorithmic architecture under a fixed training and evaluation pipeline. Given a task  $\mathcal{T}$  and an evaluation budget  $B$  (the maximum number of candidates that can be fully trained and evaluated) (Zoph & Le, 2017b; Real et al., 2017; Liu et al., 2019), each executable candidate is scored by a black-box evaluator

$$\text{Eval}_{\mathcal{T}}(a) \rightarrow \mathbf{m}(a) = (f(a), \phi(a)), \quad (1)$$

where  $f(a)$  is the primary performance metric (e.g., OOD accuracy under the task protocol (Veličković et al., 2022)) and  $\phi(a)$  is a descriptor vector derived from resource signals (e.g., MACs and parameter count) (Mouret & Clune, 2015). We keep the training and evaluation pipeline fixed across candidates so that improvements are attributable to

architecture edits rather than changes in optimization or data processing.

We distinguish between proposed candidates and evaluated candidates. A proposed candidate is produced by the LLM editor. Only candidates that are executable and pass feasibility checks enter  $\text{Eval}_{\mathcal{T}}(\cdot)$ , become evaluated candidates, and count toward the evaluation budget  $B$ . Unless otherwise specified, the seed architecture  $a_0$  is evaluated and counts toward  $B$ .

### 3.2. Structured Progressive Knowledge Activation (SPARK)

We propose Structured Progressive Knowledge Activation (SPARK), a factor-conditioned editing method that disentangles intervention target selection from factor-conditioned refinement. At iteration  $t$ , we maintain an evolution context  $\mathcal{H}_t$  summarizing the parent candidate, recent outcomes, and optional inspiration candidates sampled from an archive. SPARK progressively activates structured knowledge from  $\mathcal{H}_t$  in three stages: (i) it routes the intervention to a discrete factor (ASR, ARCHITECTURE SCOPE ROUTER), (ii) it converts recent search signals into an explicit refinement directive (RC, REFINEMENT COMPASS), and (iii) it performs a single-shot factor-conditioned code edit under the directive (SAR, SCOPED ARCHITECTURE REFINER).

**Factor-conditioned evolution step.** Each SPARK step factorizes as

$$\begin{aligned} f_t &\leftarrow \text{ASR}(a_t, \mathcal{H}_t), \\ d_t &\leftarrow \text{RC}(a_t, f_t, \mathcal{H}_t), \\ \tilde{a}_{t+1} &\leftarrow \text{SAR}(a_t, f_t, d_t, \mathcal{H}_t), \end{aligned} \quad (2)$$

where  $f_t$  is a discrete factor indicating the intervention target,  $d_t$  is a refinement directive, and  $\tilde{a}_{t+1}$  is the proposed offspring program. Intuitively, ASR answers what to intervene on (target selection), while RC+SAR specify how to revise under the chosen factor (factor-conditioned refinement).

**LLM roles and decoding.** SPARK uses a single base LLM with role-specific prompts for routing/directive/editing (denoted as  $\text{LLM}_{\text{route}}$ ,  $\text{LLM}_{\text{dir}}$ , and  $\text{LLM}_{\text{edit}}$  for clarity). All LLM calls use the same decoding hyperparameters (temperature = 0.7, other settings fixed) and we report results over multiple random seeds.

**CLRS instantiation: factorization into OPERATOR and ACTION.** In our CLRS-based architecture programs, the editable design naturally separates into two intrinsic factors

$$\mathcal{S} = \{\text{OPERATOR}, \text{ACTION}\}. \quad (3)$$

**Algorithm 1** Structured Progressive Knowledge Activation (SPARK)

---

```

1: Input: Initial architecture  $a_0$ ; factors  $\mathcal{S} = \{\text{OPERATOR, ACTION}\}$ 
2: Input: Evaluation budget  $B$ ; RC stagnation window  $k = 3$ ; proposal window  $k' = 10$ 
3: Input: Router retries  $R_{\text{asr}}$ ; archive discretizer  $b(\cdot)$ ; migration period  $P$ 
4:  $(f, \phi) \leftarrow \text{Eval}_{\mathcal{T}}(a_0)$ ; initialize islanded MAP-Elites archive  $\mathcal{D}$  with  $a_0$ 
5:  $n_{\text{eval}} \leftarrow 1$ 
6: Initialize a FIFO buffer  $\mathcal{Q}_{\text{prop}}$  to store recent proposal feasibility outcomes (size  $k'$ )
7: while  $n_{\text{eval}} < B$  do
8:   Sample parent  $a_t$  (and inspirations) from  $\mathcal{D}$ 
9:   Build context  $\mathcal{H}_t$  (parent, recent outcomes, inspirations,  $\mathcal{Q}_{\text{prop}}$  summary)
10:   $f_t \leftarrow \text{ASR}(a_t, \mathcal{H}_t, \mathcal{S}, R_{\text{asr}})$  // target selection
11:   $d_t \leftarrow \text{RC}(a_t, f_t, \mathcal{H}_t, k, k')$  // directive under factor
12:   $\tilde{a} \leftarrow \text{SAR}(a_t, f_t, d_t, \mathcal{H}_t)$  // single-shot edit
13:  if  $\tilde{a} = \text{FAIL}$  or  $\tilde{a} \notin \mathcal{F}(a_t, f_t)$  then
14:    Push FAIL (with failure type) to  $\mathcal{Q}_{\text{prop}}$ ; continue
15:  end if
16:  Push PASS to  $\mathcal{Q}_{\text{prop}}$ 
17:   $(f, \phi) \leftarrow \text{Eval}_{\mathcal{T}}(\tilde{a})$ 
18:   $n_{\text{eval}} \leftarrow n_{\text{eval}} + 1$ 
19:   $c \leftarrow b(\phi)$ ; update archive cell  $c$  if improved (tie-break by lower MACs)
20:  Migrate elites every  $P$  iterations across islands
21: end while
22: return best archived architecture(s) in  $\mathcal{D}$ 
    
```

---

OPERATOR modifies operator choices and parameterizations (e.g., projections and gating primitives), while ACTION modifies how operators are invoked and composed in the forward computation (e.g., message construction/wiring, control flow, and masking action). In the implementation, these map to two disjoint code regions in the program, while non-architectural scaffolding (public interfaces, training pipeline hooks, and task I/O) remains frozen.

**Factor-scoped tokenization (factor tokens + region tags).**

We annotate each candidate program with two disjoint code regions corresponding to OPERATOR and ACTION. Concretely, we wrap each region with fixed boundary tags (region markers) and require the LLM editor to output a complete updated program while preserving the tags. The router (ASR) emits a single factor token indicating  $f_t \in \mathcal{S}$ ; the factor token is restricted to  $\{\text{OPERATOR, ACTION}\}$  and is parsed deterministically. This design makes the edit target explicit (via factor tokens) and enables factor-locality enforcement (via region tags + feasibility checks).

**Algorithm 2** SPARK Modules: ASR, RC, and SAR

---

```

1: Procedure ASR( $a_t, \mathcal{H}_t, \mathcal{S}, R_{\text{asr}}$ )
2:   for  $r = 1$  to  $R_{\text{asr}}$  do
3:      $y \leftarrow \text{LLM}_{\text{route}}(\text{RoutePrompt}(a_t, \mathcal{H}_t))$ 
4:      $f \leftarrow \text{ParseFactor}(y)$ 
5:     if  $f \in \mathcal{S}$  then return  $f$  end if
6:   end for
7:   return ACTION

8: Procedure RC( $a_t, f_t, \mathcal{H}_t, k, k'$ )
9:   Definition (evaluated). An evaluated candidate is one that passes feasibility checks and enters  $\text{Eval}_{\mathcal{T}}(\cdot)$  (thus counted toward the budget).
10:  Compute stagnation over the last  $k$  evaluated candidates in  $\mathcal{H}_t$  (e.g., best-so-far improvement).
11:  Compute feasibility failure rate and dominant failure types over the last  $k'$  proposals using  $\mathcal{Q}_{\text{prop}}$ .
12:   $d \leftarrow \text{LLM}_{\text{dir}}(\text{DirectivePrompt}(a_t, f_t, \text{signals}))$ 
13:  return Sanitize( $d$ )

14: Procedure SAR( $a_t, f_t, d_t, \mathcal{H}_t$ )
15:   $\tilde{a} \leftarrow \text{LLM}_{\text{edit}}(\text{EditPrompt}(a_t, f_t, d_t, \mathcal{H}_t))$ 
16:  if HasRegionTags( $\tilde{a}$ ) then return  $\tilde{a}$  end if
17:  return FAIL
    
```

---

**3.3. Factor-Respecting Feasibility**

We define the factor-local feasible set for a parent  $a_t$  and factor  $f_t$  as

$$\mathcal{F}(a_t, f_t) \triangleq \left\{ a \in \mathcal{A} \mid \begin{array}{l} \text{Edit}(a, a_t) \subseteq \mathcal{R}_{f_t}, \\ a \models \mathcal{E}_{f_t} \wedge \mathcal{C} \end{array} \right\}, \quad (4)$$

where  $\mathcal{R}_{f_t}$  is the editable code region for factor  $f_t$ ,  $\mathcal{E}_{f_t}$  denotes template/schema constraints (preserve boundary tags, edit only the designated region, and output a syntactically complete program), and  $\mathcal{C}$  denotes semantic constraints shared across factors (interface invariants and tensor-shape/masking requirements). Importantly,  $\mathcal{C}$  is factor-invariant.

**Operationalizing edits and regions.** We compute  $\text{Edit}(a, a_t)$  as a line-based diff over a normalized code representation. Normalization is purely formatting-level: we (i) normalize line endings to LF, and (ii) strip trailing whitespaces on each line; no semantic code transformation (e.g., comment removal, import reordering) is performed. We map changed line ranges to regions using the fixed boundary tags that delimit  $\mathcal{R}_{\text{OPERATOR}}$  and  $\mathcal{R}_{\text{ACTION}}$ . A proposal is accepted only if all modified lines fall within the selected region  $\mathcal{R}_{f_t}$  and the entire non-selected region text (between boundary tags) is byte-identical to the parent after normalization.

**Feasibility pipeline.** In practice, we enforce  $\tilde{a}_{t+1} \in \mathcal{F}(a_t, f_t)$  using a lightweight feasibility pipeline: (1) syntax

check (parse/import of the generated program), (2) interface check (frozen signatures and required symbols are present and unchanged), and (3) semantic check (a forward-only pass under the CLRS input specification to validate tensor shapes and masking invariants, including correct handling of adjacency-defined non-edges). This pipeline is orders of magnitude cheaper than full training. Candidates failing any check are rejected before evaluation and do not count toward the evaluation budget; remaining training instabilities (if any) are reflected by  $\text{Eval}_{\mathcal{T}}(\cdot)$ .

### 3.4. Search Backbone and Overall Procedure

**Backbone-agnostic interface.** SPARK consists of a factor-conditioned editing operator (Sec. 3.2) and feasibility enforcement (Sec. 3.3). It can be integrated into any multi-round search procedure that (i) selects a parent architecture (optionally with inspirations) and (ii) evaluates the edited candidate to provide fitness feedback. The search backbone only affects the sampling policy across rounds; our contribution is the SPARK operator itself.

**Backbone used in experiments.** In this paper, we instantiate the search loop with an archive-based evolutionary backbone (OpenEvolve) (Sharma, 2025), which maintains an archive of elites and replaces an incumbent when a new candidate achieves higher fitness. We use the default OpenEvolve settings unless otherwise specified.

Algorithm 1 summarizes the overall pipeline under this instantiation, and Algorithm 2 details the three SPARK modules.

## 4. Experiments and Results

We evaluate **Structured Progressive Knowledge Activation (SPARK)** on the CLRS Algorithmic Reasoning Benchmark (Veličković et al., 2022), following the same benchmark family considered by EvoPrompting (Chen et al., 2023). Our primary controlled comparison is between **OpenEvolve (OE)** and **SPARK** under an identical search backbone and an identical LLM editor, so that differences are attributable to SPARK’s where-then-how, factor-scoped evolution operator rather than the underlying evolutionary infrastructure or language model.

Unless otherwise specified, the evolutionary loop is built on OpenEvolve (Sharma, 2025), and the generator/editor is DeepSeek-R1-0528 (DeepSeek, 2025) accessed via an OpenAI-compatible API endpoint. We treat the LLM as a black-box code editor: we use a single prompt template throughout, with no prompt-tuning, no multi-prompt rounds, and no model-side adaptation. Search is initialized from the canonical CLRS reference implementation, and candidates are obtained by iterative edits of this single seed program

(without changing the underlying model family), which reduces confounding human priors from multi-seed initialization and isolates the effect of SPARK’s factor-scoped edits.

To encourage diversity, we use an island-based population (5 islands, population size 100) with an in-memory archive of size 100. We discretize archive cells using descriptors over  $\{\text{ood\_acc}, \text{macs}\}$ . At each iteration, the prompt includes both exploitation and exploration context by inserting the top-performing programs (5) and a set of diverse programs (5) sampled from the archive. We enable cascade evaluation to filter clearly poor candidates before full evaluation (threshold  $-100$ ), and use robust request handling (timeouts and retries) to reduce interruptions during long runs.

### Budget accounting: proposal attempts vs. evaluations.

We distinguish proposal attempts (LLM edit calls; indexed by iteration) from evaluations. A candidate counts as one evaluation only if it is executable and passes feasibility checks, and is then fully trained and scored under the CLRS protocol. Non-executable proposals are rejected and therefore do not count as evaluations. Accordingly, our reliability curves (Fig. 2) report metrics over a fixed 100-attempt trajectory, while our evaluation-efficiency statement (consistent with the Abstract/Introduction) is reported in terms of the number of evaluated candidates.

**Search vs. transfer protocol.** For computational comparability, we perform architecture evolution only on DFS and then transfer the best-found architecture to the remaining CLRS tasks without task-specific evolution. In contrast, EvoPrompting performs evolution across multiple tasks. Under this setting, strong performance on the non-DFS tasks reflects the cross-task generalization of the evolved architecture and the robustness of SPARK’s search dynamics.

All candidates are trained and evaluated under the standard CLRS protocol (Veličković et al., 2022). We report OOD accuracy and MACs, and analyze search efficiency and reliability by tracking best-so-far progress, entanglement, and executability as a function of proposal attempts and evaluated candidates.

### 4.1. CLRS architecture

We evaluate SPARK on the CLRS algorithmic reasoning benchmark (Veličković et al., 2022), a standardized suite designed to test whether neural networks can learn algorithmic reasoning across a diverse set of classical algorithms drawn from standard curricula (Cormen et al., 2009). CLRS is particularly suitable for studying multi-round LLM-driven evolution because it requires systematic generalization beyond pattern matching: models must infer and execute algorithmic computation over structured inputs, rather than

Table 1. Comparison of model size (MACs) and OOD accuracy on select CLRS tasks (Veličković et al., 2022). We report results for the CLRS reference architecture (CLRS), OpenEvolve (OE) (Sharma, 2025), EvoPrompting (EP) (Chen et al., 2023), FunSearch (FS) (Romera-Paredes et al., 2024), EoH (Liu et al., 2024a), and our method (Ours; i.e., SPARK), including a single-iteration variant (Ours-lit). Our model size is measured by MACs and can be viewed as the CLRS reference compute plus a small, fixed overhead introduced by the SPARK editing interface, which is constant across tasks. Therefore, gains in OOD accuracy mainly stem from improved search dynamics enabled by factor-isolated edits (operator vs. action), rather than increased capacity/compute. **Abbreviations:** AP=Articulation Points, QS=Quickselect, CC=Connected Components, AS=Activity Selector, FMS=Find Maximum Subarray (Kadane), Dij=Dijkstra, LCS=LCS Length, Min=Minimum, TS=Topological Sort.

Metric / Method	CLRS task (abbr.)											
	DFS	AP	QS	CC	AS	FMS	Dij	LCS	Min	TS	Avg.	
MACs (K)	CLRS	661	532	396	663	262	265	526	270	261	660	450
	OE	693	563	427	695	294	296	557	302	293	692	481
	EP	660	498	377	707	262	261	525	270	260	660	448
	FS	680	551	415	683	282	284	545	290	281	679	469
	EoH	675	546	410	677	276	278	540	284	275	674	463
	Ours-lit	670	541	405	673	271	274	535	280	271	669	459
	Ours	664	535	399	666	265	268	529	273	264	663	453
OOD acc.(%)	CLRS	46.78	88.32	0.47	43.43	95.18	76.36	96.05	80.51	97.78	87.27	71.22
	OE	32.54	61.32	3.71	45.21	95.43	77.05	95.85	87.53	98.10	86.31	68.30
	EP	68.14	93.46	0.79	41.86	95.05	75.35	97.30	85.75	98.40	88.12	74.42
	FS	74.50	94.07	1.49	62.08	95.61	77.75	96.84	82.93	97.91	92.88	77.61
	EoH	77.27	95.03	4.25	65.90	96.22	80.51	97.44	84.56	98.14	95.00	79.43
	Ours-lit	45.60	73.04	9.57	51.56	97.54	79.79	97.80	86.89	99.02	84.94	72.58
	Ours	<b>83.74</b>	<b>97.90</b>	<b>10.69</b>	<b>77.34</b>	<b>98.03</b>	<b>85.64</b>	<b>99.22</b>	<b>87.60</b>	<b>99.07</b>	<b>99.95</b>	<b>83.92</b>

relying on superficial correlations or short-horizon heuristics. Following prior work, we view success on CLRS as evidence of improved algorithmic alignment—the ability to solve problems by reasoning in a manner consistent with the underlying computation graph of the target algorithm (Xu et al., 2020).

**Benchmark structure.** In CLRS, each algorithmic instance is represented as a graph-structured input, and the algorithm is expressed as a trajectory of operations over this graph (e.g., node/edge updates and readouts) (Veličković et al., 2022). This formulation naturally supports message-passing models and allows evaluation across a broad set of algorithms under a shared interface. Prior studies have shown that graph neural networks can process such trajectories effectively, and that carefully designed message-passing architectures can provide strong performance across many CLRS tasks (Ibarz et al., 2022; Gilmer et al., 2017).

**Architecture instantiation and search target.** To isolate the effect of multi-round evolution from changes in model family, we operate directly on the original CLRS reference architecture provided by the benchmark (Veličković et al., 2022). That is, our search starts from the official reference implementation and iteratively edits its Python function definition. As illustrated in Fig. 1, this code-based representation exposes two intrinsic, disjoint architecture factors: (i) **OPERATOR** (module parameter-

ization/structure definitions, e.g., components defined in `__init__`), and (ii) **ACTION** (how operators are composed, reused, masked, and routed in `forward`). SPARK implements a where-then-how evolution operator that factorizes each update into: where = discrete scope selection over {OPERATOR, ACTION} (ASR), followed by how = within-scope refinement under an explicit directive (RC+SAR). This separation is designed to reduce cross-factor interference and make improvements more composable across iterations.

## 4.2. Main Results on CLRS

### Evaluation protocol (DFS search; reporting on 10 tasks).

For each method, we run an LLM-driven evolutionary search on the CLRS `dfs` task for 100 proposal attempts under the same search budget and evaluation harness, and measure OOD accuracy using the CLRS OOD split. We then take the incumbent best architecture discovered on `dfs` and train/evaluate it from scratch on an additional 9 representative CLRS tasks. We report (i) per-task OOD accuracy and MACs on these 10 tasks (Table 1), and (ii) reliability/progress curves over the 100-attempt trajectory (Fig. 2). (Full results over all CLRS tasks are provided in the appendix.)

**Baselines and reproducibility.** We compare against EvoPrompting (Chen et al., 2023), OpenEvolve (Sharma, 2025), FunSearch (Romera-Paredes et al., 2024), and EoH (Liu

et al., 2024a) (as listed in Table 1). Since the OpenEvolve and FunSearch papers do not explicitly report results on CLRS, we obtain their CLRS numbers by running their released code in our CLRS pipeline, using the same dfs-based evolution setting and the same 100-attempt budget as SPARK for a fair controlled comparison.

**Evaluation-efficiency reporting (consistent with Abstract/Introduction).** On dfs, SPARK reaches its best OOD accuracy (83.74%) by proposal attempt 57, corresponding to 57 evaluated candidates in that run. This already surpasses EvoPrompting’s best DFS result under its 1600-evaluation setting, yielding a  $1600/57 \approx 28.1\times$  improvement in evaluation efficiency.

Table 1 summarizes OOD accuracy and model size (MACs) on representative CLRS tasks. Across all listed tasks, SPARK (Ours) achieves the best OOD accuracy, consistently outperforming the CLRS reference architecture as well as strong LLM-evolution baselines (OE/EP/FS/EoH), indicating that structure-guided, factor-scoped editing supports more reliable multi-round progress under the same proposal budget. The gains are particularly pronounced on graph-reasoning tasks: on DFS we improve from 46.78 (CLRS) / 74.50 (FS) to 83.74 (Ours), and on CC from 43.43 (CLRS) / 62.08 (FS) to 77.34. We also observe substantial relative gains in regimes where the reference model performs poorly, e.g., QS (0.47  $\rightarrow$  10.69), highlighting the benefit of controlling where to edit before generating how to edit.

The single-iteration variant (Ours-1it) already improves over CLRS on several tasks (e.g., QS: 0.47  $\rightarrow$  9.57), but remains clearly behind Ours (QS: 10.69; DFS: 83.74), supporting the necessity of multi-round evolution for sustained gains.

Importantly, these improvements are not explained by capacity/compute scaling. As shown by the MACs in Table 1, Ours stays close to the CLRS reference compute across tasks (e.g., 661K vs. 664K on DFS; 663K vs. 666K on CC), and is often comparable to or smaller than the baselines. Therefore, the accuracy gains primarily reflect improved search dynamics induced by factor-scoped updates rather than increased compute.

Finally, tasks that require multi-step, compositional reasoning (e.g., DFS, CC, and TS) benefit most, with TS reaching 99.95 (Ours) compared to 87.27 (CLRS) and 92.88 (FS), consistent with our hypothesis that reducing cross-factor entanglement improves iterative search stability.

**4.3. Ablation on Factorized Editing**

**Ablation on factorized edits (ASR vs. RC+SAR) on DFS.** SPARK factorizes each evolution step into ASR (scope selection) and RC+SAR (scope-local refinement). Table 2

Table 2. DFS ablation (CLRS): ASR vs. RC+SAR under different LLM editors. We compare using only RC+SAR, only ASR, and full SPARK (ASR+RC+SAR) with identical evaluation protocol. OOD is OOD accuracy on DFS over valid (evaluable) proposals;  $\Delta$  is the gain (pp) over the CLRS baseline.

Variant	LLM	MACs↓	OOD↑	$\Delta$ ↑
CLRS (base)	DeepSeek-R1	661,190	46.78	+0.00
RC+SAR only	DeepSeek-R1	727,823	56.79	+10.01
ASR only	DeepSeek-R1	693,926	65.28	+18.50
Ours (SPARK)	DeepSeek-R1	664,157	<b>83.74</b>	<b>+36.96</b>
RC+SAR only	Qwen-Plus	731,000	56.00	+9.22
ASR only	Qwen-Plus	697,000	64.50	+17.72
Ours (SPARK)	Qwen-Plus	665,308	<b>80.50</b>	<b>+33.72</b>

reports DFS results under two LLM editors (DeepSeek-R1 and Qwen-Plus). With DeepSeek-R1, using only RC+SAR yields a modest improvement over the CLRS baseline (46.78 $\rightarrow$ 56.79, +10.01 pp), while using only ASR brings a larger gain (46.78 $\rightarrow$ 65.28, +18.50 pp), suggesting that correctly localizing the intervention scope is more critical than refinement alone. Combining ASR and RC+SAR (SPARK) achieves the best accuracy (83.74, +36.96 pp) with MACs close to the reference (664K vs. 661K), indicating the gains are not driven by capacity scaling. We observe the same qualitative trend with Qwen-Plus: RC+SAR only improves to 56.00 (+9.22 pp) and ASR only reaches 64.50 (+17.72 pp), whereas SPARK attains 80.50 (+33.72 pp) with comparable MACs (665K).

**4.4. Search Dynamics and Reliability**

These ablations also explain the reliability patterns in Fig. 2. ASR explicitly constrains edits to a single scope, which reduces cross-scope entanglement (Fig. 2b) and in turn increases the fraction of proposals that remain executable and evaluable (Fig. 2c). As a result, more of the fixed 100-attempt budget is converted into effective optimization steps, yielding faster and higher best-so-far OOD accuracy (Fig. 2a). RC+SAR alone can refine locally once a good scope is implicitly hit, but without reliable scope localization it is more likely to produce edits whose effects are harder to attribute or that interfere with other architectural factors, which aligns with the higher entanglement and lower validity observed for unconstrained editing. Overall, separating scope selection (ASR) from within-scope refinement (RC+SAR) reduces entanglement, improves executability, and leads to more reliable multi-round progress.

**Why functional entanglement hurts multi-round search.**

Multi-round evolution benefits from making small, attributable changes that can compose across iterations. When an edit touches multiple scopes (or leaks into frozen scaffolding), it effectively introduces multiple coupled constraints

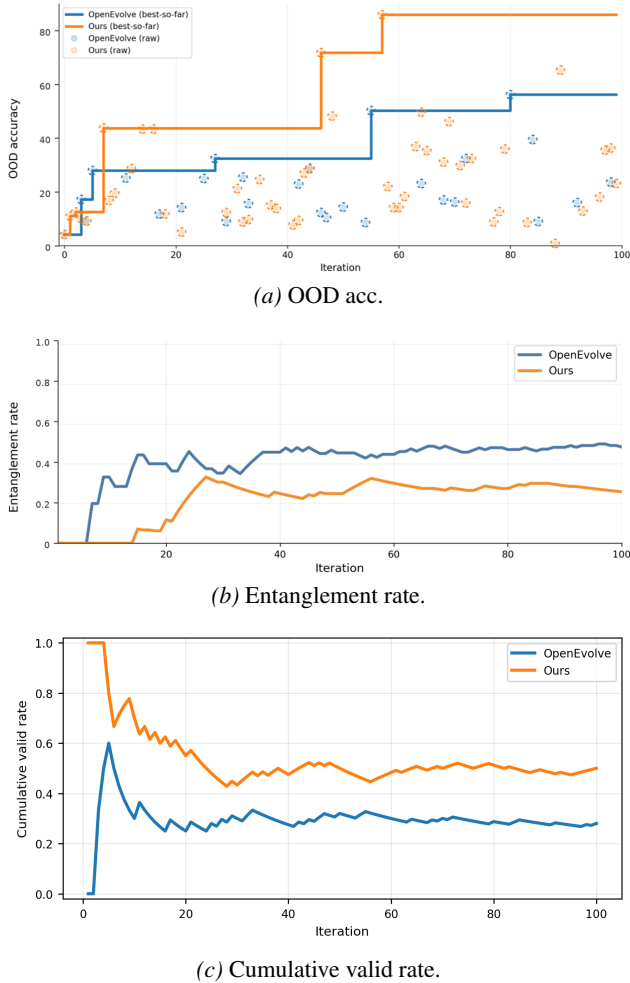


Figure 2. SPARK vs. OpenEvolve under a 100-attempt budget: (a) best-so-far OOD accuracy over valid (evaluable) candidates, (b) entanglement rate measured by non-factor-local (cross-scope) edits, and (c) cumulative valid rate (executability). Together, lower entanglement increases the fraction of evaluable proposals and accelerates best-so-far accuracy gains.

at once, increasing the chance of violating interface/shape requirements and reducing the fraction of proposals that remain evaluable. A simple way to see this is to model feasibility as a per-scope event: if changing one scope preserves executability with probability  $p_v$ , then an entangled edit affecting  $k$  scopes has feasibility approximately  $p_v^k$ , which drops quickly as  $k$  increases. Moreover, coupled multi-scope changes confound credit assignment: even if one local modification is beneficial, side effects from other touched regions can cancel the gain or destabilize training, reducing the probability that improvements are retained and amplified across rounds. This motivates enforcing scope-local edits (via ASR) before applying within-scope refinement (via RC+SAR), which directly targets lower entanglement, higher validity, and more reliable best-so-far progress as observed in Fig. 2.

**Functional entanglement rate.** Fig. 2b reports the entanglement rate during search. We define an edit as entangled if its code diff is not factor-local: it modifies both functional factor regions (Operator and Action) in the same revision, or touches any frozen scaffolding outside these regions (e.g., interfaces/I/O hooks). Operationally, we compute a normalized line-based diff between a parent and its offspring and check which predefined code regions the changed lines fall into; the exact criterion and region definitions are provided in Appendix. Compared with OpenEvolve, SPARK yields a consistently lower entanglement rate, indicating fewer mixed-factor or scaffolding-touching revisions

**Reliability of proposal generation.** Fig. 2c evaluates reliability under a fixed 100-attempt budget via the cumulative valid rate, where a proposal is valid if it compiles/runs and passes feasibility checks to enter scoring. SPARK maintains a substantially higher valid rate throughout the trajectory (stabilizing around 0.5–0.6 by iteration 100) than OpenEvolve (around 0.25–0.3), meaning a larger fraction of attempts become evaluable candidates. This improvement aligns with the lower entanglement rate: cross-factor or scaffolding-touching edits are more likely to violate interface/shape constraints and fail before evaluation.

**Search progress under a fixed attempt budget.** Fig. 2a plots best-so-far OOD accuracy over valid candidates. Under the same 100 attempts, SPARK improves faster and reaches 83.74 at iteration 57, while OpenEvolve peaks later (around iteration 80). Taken together, Figs. 2a–2c suggest a tight coupling between entanglement, executability, and progress: reducing entanglement tends to increase the fraction of evaluable proposals, which makes a larger portion of the fixed attempt budget effective for improving best-so-far accuracy.

The supplementary material reports per-task results on all 18 CLRS tasks, including full accuracy tables beyond the main text. It also includes multi-seed experiments and complete evolution traces (the discovered architectures and best-so-far trajectories across iterations) to further support the reliability and sample-efficiency claims.

## 5. Conclusion

We study LLM-driven neural architecture search as multi-round evolution over executable programs and identify cross-factor functional entanglement as a key reliability bottleneck. We propose SPARK, which enables factor-isolated editing via factor selection and factor-conditioned patch generation, instantiated on CLRS with Operator/Action factors and feasibility checks.

On CLRS, SPARK improves over the reference on 12/18 tasks and outperforms EvoPrompting on 10/18, reaching

83.74% OOD on DFS with 57 evaluated candidates for a  $28.1\times$  speedup under our evaluation accounting.

## 6. Impact Statement

This paper presents work whose goal is to advance the reliability of LLM-driven architecture evolution and neural architecture search. While the techniques studied here may improve the efficiency and reproducibility of model development, we do not anticipate direct negative societal impacts beyond those commonly associated with general-purpose machine learning research.

## References

- Chen, A., Dohan, D. M., and So, D. R. Evoprompting: Language models for code-level neural architecture search. *arXiv preprint arXiv:2302.14838*, 2023. URL <https://arxiv.org/abs/2302.14838>.
- Cormen, T. H., Leiserson, C. E., Rivest, R. L., and Stein, C. *Introduction to Algorithms, 3rd Edition*. MIT Press, 2009. ISBN 978-0-262-03384-8. URL <http://mitpress.mit.edu/books/introduction-algorithms>.
- DeepSeek. Deepseek-r1-0528 release notes. <https://api-docs.deepseek.com/news/news250528>, 2025. Accessed 2026-01-21.
- Dong, X. and Yang, Y. Nas-bench-201: Extending the scope of reproducible neural architecture search. In *International Conference on Learning Representations (ICLR)*, 2020. URL <https://arxiv.org/abs/2001.00326>.
- Fernando, C., Banarse, D., Michalewski, H., Osindero, S., and Rocktäschel, T. Promptbreeder: Self-referential self-improvement via prompt evolution. In *International Conference on Learning Representations (ICLR)*, 2024. URL <https://arxiv.org/abs/2309.16797>.
- Fu, J., Zhu, X., and Li, Y. Recognition of surface defects on steel sheet using transfer learning. *arXiv preprint arXiv:1909.03258*, 2019.
- Fu, J., Wang, B., Zhang, H., Zhang, Z., Chen, W., and Zheng, N. When and why momentum accelerates sgd: An empirical study. *arXiv preprint arXiv:2306.09000*, 2023a.
- Fu, J., Yang, T., Wang, Y., Lu, Y., and Zheng, N. Breaking through the learning plateaus of in-context learning in transformer. *arXiv preprint arXiv:2309.06054*, 2023b.
- Fu, J., Zhang, X., Wang, Y., Zeng, W., and Zheng, N. Understanding mobile gui: From pixel-words to screen-sentences. *Neurocomputing*, 601:128200, 2024.
- Gilmer, J., Schoenholz, S. S., Riley, P. F., Vinyals, O., and Dahl, G. E. Neural message passing for quantum chemistry. In Precup, D. and Teh, Y. W. (eds.), *Proceedings of the 34th International Conference on Machine Learning*, volume 70 of *Proceedings of Machine Learning Research*, pp. 1263–1272. PMLR, 06–11 Aug 2017. URL <https://proceedings.mlr.press/v70/gilmer17a.html>.
- Gupta, R., Pal, S., Kanade, A., and Shevade, S. Deepfix: Fixing common C language errors by deep learning. In *Proceedings of the Thirty-First AAAI Conference on Artificial Intelligence*, pp. 1345–1351, San Francisco, California, USA, 2017. AAAI Press.
- Hemberg, E. and O’Reilly, U.-M. Evolving code with a large language model. *arXiv preprint arXiv:2401.07102*, 2024. URL <https://arxiv.org/abs/2401.07102>.
- Ibarz, B., Kurin, V., Papamakarios, G., Nikiforou, K., Benani, M., Csordás, R., Dudzik, A. J., Bošnjak, M., Vitvitskyi, A., Rubanova, Y., Deac, A., Bevilacqua, B., Ganin, Y., Blundell, C., and Veličković, P. A generalist neural algorithmic learner. In Rieck, B. and Pascanu, R. (eds.), *Proceedings of the First Learning on Graphs Conference*, volume 198 of *Proceedings of Machine Learning Research*, pp. 2:1–2:23. PMLR, 09–12 Dec 2022. URL <https://proceedings.mlr.press/v198/ibarz22a.html>.
- Ji, Z., Zhu, G., Yuan, C., and Huang, Y. RZ-NAS: Enhancing LLM-guided neural architecture search via reflective zero-cost strategy. In *Proceedings of the 42nd International Conference on Machine Learning*, volume 267 of *Proceedings of Machine Learning Research*, pp. 27237–27254, 2025. URL <https://proceedings.mlr.press/v267/ji25a.html>.
- Lehman, J., Gordon, J., Jain, S., Ndousse, K., Yeh, C., and Stanley, K. O. Evolution through large models. *arXiv preprint arXiv:2206.08896*, 2022. URL <https://arxiv.org/abs/2206.08896>.
- Li, P., Wu, K., Huang, W., Zhou, S., and Wang, J. Camera-aware label refinement for unsupervised person re-identification. *arXiv preprint arXiv:2403.16450*, 2024.
- Li, P., Wu, K., Fu, J., and Zhou, S. Regnav: Room expert guided image-goal navigation. In *Proceedings of the AAAI Conference on Artificial Intelligence*, volume 39, pp. 4860–4868, 2025a.
- Li, Z., Lin, Z., and Wang, Y. Collm-nas: Collaborative large language models for efficient knowledge-guided neural architecture search. *arXiv preprint arXiv:2509.26037*, 2025b. URL <https://arxiv.org/abs/2509.26037>.

- Liu, F., Tong, X., Yuan, M., Lin, X., Luo, F., Wang, Z., Lu, Z., and Zhang, Q. Evolution of heuristics: Towards efficient automatic algorithm design using large language model. In Salakhutdinov, R., Kolter, Z., Heller, K., Weller, A., Oliver, N., Scarlett, J., and Berkenkamp, F. (eds.), *Proceedings of the 41st International Conference on Machine Learning*, volume 235 of *Proceedings of Machine Learning Research*, pp. 32201–32223. PMLR, 21–27 Jul 2024a. URL <https://proceedings.mlr.press/v235/liu24bs.html>.
- Liu, H., Simonyan, K., and Yang, Y. Darts: Differentiable architecture search. In *International Conference on Learning Representations*, 2019. URL <https://openreview.net/forum?id=S1eYHoC5FX>.
- Liu, Y., Huang, Q., Hui, S., Fu, J., Zhou, S., Wu, K., Li, P., and Wang, J. Semantic-aware representation learning for homography estimation. In *Proceedings of the 32nd ACM International Conference on Multimedia*, pp. 2506–2514, 2024b.
- Liu, Y., Fu, J., Wu, Y., Wu, K., Li, P., Wu, J., Zhou, S., and Xin, J. Mind the gap: Aligning vision foundation models to image feature matching. In *Proceedings of the IEEE/CVF International Conference on Computer Vision*, pp. 20313–20323, 2025.
- Madaan, A., Tandon, N., et al. Self-refine: Iterative refinement with self-feedback. *arXiv preprint arXiv:2303.17651*, 2023. URL <https://arxiv.org/abs/2303.17651>.
- Meyerson, E. and Miikkulainen, R. Language model crossover: Variation through few-shot prompting. *arXiv preprint arXiv:2302.12170*, 2023. URL <https://arxiv.org/abs/2302.12170>.
- Mouret, J.-B. and Clune, J. Illuminating search spaces by mapping elites. *arXiv preprint arXiv:1504.04909*, 2015.
- Nasir, M. U., Earle, S., Togelius, J., James, S., and Cleghorn, C. Llmatic: Neural architecture search via large language models and quality diversity optimization. In *Genetic and Evolutionary Computation Conference (GECCO)*, 2024. URL <https://dl.acm.org/doi/abs/10.1145/3638529.3654017>.
- Pham, H., Guan, M. Y., Zoph, B., Le, Q. V., and Dean, J. Efficient neural architecture search via parameter sharing. In *International Conference on Machine Learning (ICML)*, 2018. URL <https://arxiv.org/abs/1802.03268>.
- Qi, Y., Fu, P., Li, H., Liu, Y., Jiang, C., Qin, B., Luo, Z., and Luan, J. Patchcue: Enhancing vision-language model reasoning with patch-based visual cues. *arXiv preprint arXiv:2603.05869*, 2026.
- Rabinovich, M., Stern, M., and Klein, D. Abstract syntax networks for code generation and semantic parsing. In *Proceedings of the 55th Annual Meeting of the Association for Computational Linguistics (Volume 1: Long Papers)*, pp. 1139–1149, Vancouver, Canada, July 2017. Association for Computational Linguistics. doi: 10.18653/v1/P17-1105. URL <https://aclanthology.org/P17-1105/>.
- Real, E., Moore, S., Selle, A., Saxena, S., Suematsu, Y. L., Tan, J., Le, Q. V., and Kurakin, A. Large-scale evolution of image classifiers. In *Proceedings of the 34th International Conference on Machine Learning*, volume 70 of *Proceedings of Machine Learning Research*, pp. 2902–2911. PMLR, 2017. URL <https://proceedings.mlr.press/v70/real17a.html>.
- Real, E., Aggarwal, A., Huang, Y., and Le, Q. V. Regularized evolution for image classifier architecture search. In *AAAI Conference on Artificial Intelligence (AAAI)*, 2019. URL <https://arxiv.org/abs/1802.01548>.
- Romera-Paredes, B., Barekatin, M., Novikov, A., Balog, M., Kumar, M. P., Dupont, E., Ruiz, F. J. R., Ellenberg, J. S., Wang, P., Fawzi, O., Kohli, P., and Fawzi, A. Mathematical discoveries from program search with large language models. *Nature*, 625(7995):468–475, jan 2024. doi: 10.1038/s41586-023-06924-6.
- Sharma, A. Openevolve: an open-source evolutionary coding agent, 2025. URL <https://github.com/algorithmicsuperintelligence/openevolve>.
- Shinn, N., Cassano, F., et al. Reflexion: Language agents with verbal reinforcement learning. *arXiv preprint arXiv:2303.11366*, 2023. URL <https://arxiv.org/abs/2303.11366>.
- Veličković, P., Badia, A. P., Budden, D., Pascanu, R., Banino, A., Dashevskiy, M., Hadsell, R., and Blundell, C. The CLRS algorithmic reasoning benchmark. In *Proceedings of the 39th International Conference on Machine Learning*, volume 162 of *Proceedings of Machine Learning Research*, pp. 22084–22102. PMLR, 2022. URL <https://proceedings.mlr.press/v162/velickovic22a.html>.
- Šurina, J. et al. Algorithm discovery with large language models. *OpenReview preprint*, 2025. URL <https://openreview.net/forum?id=dNW3RGW0gi>.
- Wang, B., Fu, J., Zhang, H., Zheng, N., and Chen, W. Closing the gap between the upper bound and lower bound of adam’s iteration complexity. *Advances in Neural Information Processing Systems*, 36:39006–39032, 2023.

- Wu, K., Li, P., Fu, J., Li, Y., Wu, Y., Liu, Y., Wang, J., and Zhou, S. Event-equalized dense video captioning. In *Proceedings of the IEEE/CVF Conference on Computer Vision and Pattern Recognition*, pp. 8417–8427, 2025a.
- Wu, S. et al. Gpt-nas: Neural architecture search with large language models. *arXiv preprint arXiv:2305.05351*, 2023. URL <https://arxiv.org/abs/2305.05351>.
- Wu, X., Wu, S.-h., Wu, J., Feng, L., and Tan, K. C. Evolutionary computation in the era of large language model: Survey and roadmap. *IEEE Transactions on Evolutionary Computation*, 29(2):534–554, 2025b. doi: 10.1109/TEVC.2024.3506731. URL <https://arxiv.org/abs/2401.10034>.
- Wu, Y., Deng, Y., Zhou, S., Liu, Y., Huang, W., and Wang, J. Cr-former: Single-image cloud removal with focused taylor attention. *IEEE Transactions on Geoscience and Remote Sensing*, 62:1–14, 2024.
- Xu, K., Zhang, M., Li, J., Du, S. S., Kawarabayashi, K.-i., and Jegelka, S. How neural networks extrapolate: From feedforward to graph neural networks, 2020. URL <https://arxiv.org/abs/2009.11848>.
- Yang, C., Wang, X., Lu, Y., Liu, H., Le, Q. V., Zhou, D., and Chen, X. Large language models as optimizers. In *International Conference on Learning Representations (ICLR)*, 2024. URL <https://arxiv.org/abs/2309.03409>.
- Yin, P. and Neubig, G. A syntactic neural model for general-purpose code generation. In *Proceedings of the 55th Annual Meeting of the Association for Computational Linguistics (Volume 1: Long Papers)*, pp. 440–450, Vancouver, Canada, July 2017. Association for Computational Linguistics. doi: 10.18653/v1/P17-1041. URL <https://aclanthology.org/P17-1041/>.
- Zheng, M., Su, X., You, S., Wang, F., Qian, C., Xu, C., and Albanie, S. Can gpt-4 perform neural architecture search? *arXiv preprint arXiv:2304.10970*, 2023. URL <https://arxiv.org/abs/2304.10970>.
- Zhou, X., Wu, X., Feng, L., Lu, Z., and Tan, K. C. Design principle transfer in neural architecture search via large language models. In *AAAI Conference on Artificial Intelligence (AAAI)*, 2025. URL <https://arxiv.org/abs/2408.11330>.
- Zoph, B. and Le, Q. V. Neural architecture search with reinforcement learning. In *International Conference on Learning Representations (ICLR)*, 2017a. URL <https://arxiv.org/abs/1611.01578>.
- Zoph, B. and Le, Q. V. Neural architecture search with reinforcement learning. In *International Conference on Learning Representations*, 2017b. URL <https://openreview.net/forum?id=r1Ue8Hcxg>.

## A. supplementary for Structured Progressive Knowledge Activation for LLM-Driven Neural Architecture Search

### A.1. Overall Comparison with EvoPrompting on CLRS

Table A.1 reports the overall per-task performance comparison between our method and EvoPrompting on the CLRS benchmark.

#### Search dynamics under structure-guided evolution.

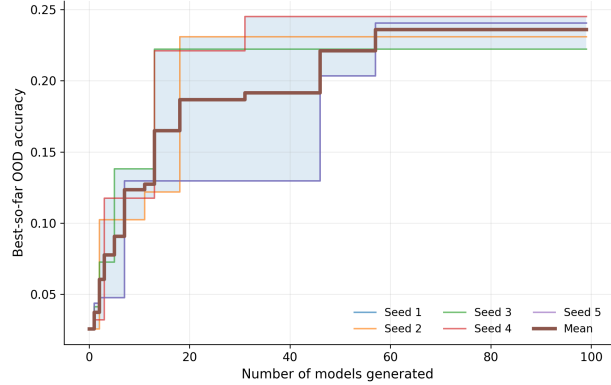
Fig. A.1 characterizes the search behavior of our Structured Progressive Knowledge Activation (SPARK) over the 100 generated candidates on CLRS, aggregated across five random seeds. Recall that SPARK factorizes each evolution step into where-to-edit and how-to-refine decisions: the Architecture Scope Router (ASR) selects an explicit scope (e.g., operator-level vs. action), the Refinement Compass (RC) specifies scope-local refinement directives, and the Scoped Architecture Refiner (SAR) applies edits only within the chosen scope under feasible-set refinement constraints (syntax/interface/shape feasibility), preventing cross-factor entanglement (Li et al., 2025a).

**Progress (best-so-far OOD accuracy).** In Fig. A.1a, the best-so-far OOD accuracy rises sharply in the early phase and then shows a saturation trend, indicating that SPARK can convert a small candidate budget into substantial performance gains, while later iterations provide more incremental improvements (Fu et al., 2023b). The thick mean curve together with the min–max band suggests this pattern is consistent across seeds rather than being driven by a single favorable run. We attribute the strong early gains to SPARK’s structured (scope-local) updates: by committing each iteration to an explicit scope via ASR and applying RC-guided, SAR-executed edits within a constrained feasible set, the search produces composable improvements that accumulate across rounds instead of being washed out by unconstrained rewrites.

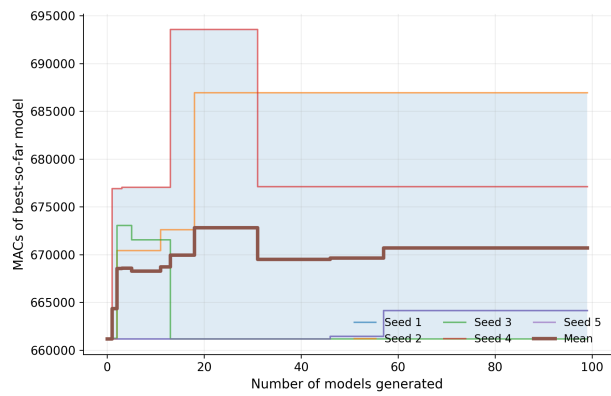
#### Cost control (MACs of the incumbent best model).

Fig. A.1b tracks the MACs of the incumbent best-so-far model throughout the same 100-attempt trajectory. Although MACs may change when the incumbent is replaced, the curves do not exhibit a systematic upward trend and remain within a stable range across seeds. This indicates that the accuracy gains in Fig. A.1a are not primarily explained by progressively increasing compute, but rather by discovering more effective structures within a comparable compute envelope—consistent with SPARK’s goal of structure-guided refinement rather than cost-increasing scaling.

**Why both plots.** We report both progress and cost because reliable multi-round LLM-driven NAS requires improvements to be (i) attributable and composable across iterations



(a) Search progress measured by best-so-far OOD accuracy.



(b) Compute footprint of the best-so-far model measured by MACs.

*Figure A.1.* Search dynamics on CLRS over 100 generated candidates (5 seeds). Lines show best-so-far trajectories per seed; the thick line is the mean and the shaded band indicates the min–max range. (a) Best-so-far OOD accuracy rises quickly then saturates. (b) Best-so-far MACs remain stable, suggesting gains come from improved structures rather than increasing compute.

(reflected by best-so-far accuracy gains) while also being (ii) cost-bounded (reflected by stable MACs). Together, Fig. A.1a and Fig. A.1b provide complementary evidence that SPARK achieves effective, budget-efficient progress without relying on an expanding computational footprint.

### A.2. Program Evolution Analysis Across Iterations

This section analyzes how the PGN triplet module evolves across iterations. We treat `maybe_lazy_init` as the Operator (parameterization/structure definition) and `compute_trimsgs` as the Action (triplet message computation). Iteration 0 is the base program we aim to evolve (Listing 1); later iterations introduce increasingly expressive, stable, and structure-aware computation (Fu et al., 2024; Wu et al., 2025a).

Table A.1. Per-task OOD accuracy (%) on 30 CLRS tasks.

Task	CLRS	EP	Ours	Task	CLRS	EP	Ours
DFS	47.8	68.1	<b>83.7</b>	MCO	<b>91.7</b>	90.8	87.3
AP	88.3	93.5	<b>97.9</b>	MPrim	86.4	<b>88.7</b>	<b>88.7</b>
QS	0.5	0.8	<b>10.7</b>	SI	97.6	<b>98.2</b>	97.1
SCC	43.4	41.9	<b>77.3</b>	BS	77.6	78.0	<b>87.6</b>
ASel	95.2	95.1	<b>98.0</b>	Br	94.0	97.6	<b>98.2</b>
FMS	76.4	75.4	<b>85.6</b>	Bub	67.7	88.9	<b>98.1</b>
Dij	96.1	97.3	<b>99.2</b>	GS	93.6	93.8	<b>96.4</b>
LCS	80.5	85.8	<b>87.6</b>	HS	31.0	69.9	<b>75.6</b>
Min	97.8	98.4	<b>99.1</b>	Ins	78.1	89.5	<b>97.5</b>
Topo	87.3	88.1	<b>99.7</b>	JM	91.0	90.4	<b>94.9</b>
BFS	99.7	<b>100.0</b>	70.6	KMP	<b>19.5</b>	16.3	14.9
FW	48.5	<b>61.4</b>	32.9	MKr	89.8	<b>91.5</b>	86.2
TSch	87.3	<b>88.2</b>	87.4	NSM	78.7	<b>79.8</b>	77.3
BFord	97.4	<b>97.5</b>	96.0	OBST	73.8	78.7	<b>96.1</b>
DSP	<b>98.2</b>	98.0	97.8	QSort	64.6	85.2	<b>97.8</b>

**Abbreviations:** AP=Articulation Points, QS=Quickselect, SCC=Strongly Connected Components, ASel=Activity Selector, FMS=Find Maximum Subarray (Kadane), Dij=Dijkstra, LCS=LCS Length, Min=Minimum, Topo=Topological Sort, BFS=Breadth-First Search, FW=Floyd–Warshall, TSch=Task Scheduling, BFord=Bellman–Ford, DSP=DAG Shortest Paths, MCO=Matrix Chain Order, MPrim=MST Prim, SI=Segments Intersect, BS=Binary Search, Br=Bridges, Bub=Bubble Sort, GS=Graham Scan, HS=Heapsort, Ins=Insertion Sort, JM=Jarvis March, KMP=KMP Matcher, MKr=MST Kruskal, NSM=Naive String Matcher, OBST=Optimal BST, QSort=Quicksort.

**Iteration 0 (Base): additive triplet construction with max aggregation.** As shown in Listing 1, the base Operator instantiates linear projections for node features ( $z$ ), edge features ( $edge\_fts$ ), and graph-level features ( $graph\_fts$ ). The base Action constructs a triplet tensor via broadcasting ( $unsqueeze$ ) and combines components primarily through additive composition followed by a max-style reduction. Benefit: this design is simple, stable, and provides a strong baseline with clear gradient paths, serving as a reliable anchor for subsequent evolution.

**Iteration 1: multi-head parameterization and explicit interaction mixing.** Compared with the base, Iteration 1 (Listing 2) evolves the Operator to a multi-head design (e.g., per-head projections and head-wise composition), enabling multiple latent “views” of triplet reasoning. In the Action, the computation moves beyond purely additive composition by introducing explicit interaction mixing terms (e.g., node–node, node–edge, and edge–edge interactions) before head fusion. Benefit: richer compositional expressivity—multiple heads can capture diverse relational patterns and reduce the bottleneck of a single projection path (Liu et al., 2024b).

**Iteration 2: residual augmentation for more stable learning.** Iteration 2 (Listing 3) keeps the base-style aggregation backbone but introduces a residual pathway in the Action, injecting an additional direct mapping (from a selected intermediate component) into the output. Benefit: improved optimization stability—when triplet aggregation

is uncertain early in training, the residual provides a reliable shortcut signal, mitigating under-training of deep interaction paths (Fu et al., 2023a; Wang et al., 2023).

**Iteration 7: gated residual injection to suppress noisy edges.** Building on Iteration 2, Iteration 7 (Listing 4) adds a gating mechanism on the residual branch, so the residual contribution becomes evidence-dependent rather than always-on. Benefit: better robustness—noisy or low-confidence edges are less likely to dominate the message update, while informative edges retain strong influence (Li et al., 2024).

**Iteration 46: structure-aware masking and multi-statistic aggregation.** Iteration 46 (Listing 5) introduces a structural prior into the Action by incorporating an adjacency mask (e.g.,  $adj\_mat$ ) to constrain where messages are valid, effectively preventing propagation along non-existent edges. It also enriches the aggregation by combining complementary statistics (e.g., max- and mean-style summaries) followed by a learned mixer (Wu et al., 2024; Qi et al., 2026). Benefit: (i) improved structural consistency—messages respect the graph topology; (ii) more robust summarization—max captures salient evidence while mean stabilizes noisy activations.

**Iteration 57: context-conditioned channel gating for node/edge/global streams.** Iteration 57 (Listing 6) evolves the Operator into a more adaptive form by adding fine-grained gates over the node, edge, and global feature

streams, making projections condition-dependent. The Action correspondingly applies these gates to modulate which channels/branches are emphasized under different inputs, and further conditions residual control on richer context. Benefit: strong adaptivity and generalization—dynamic channel selection acts as a soft routing mechanism, allowing the module to emphasize the most relevant relational cues under varying structural and contextual conditions (Liu et al., 2025; Fu et al., 2019).

**Overall trend.** Starting from the base (Iteration 0), the evolution follows a clear trajectory: (1) expressivity via multi-head and interaction mixing (Iteration 1), (2) stability via residual and gated residual designs (Iterations 2 and 7), and (3) validity & adaptivity via topology-aware masking and context-conditioned gating (Iterations 46 and 57). These changes progressively strengthen the Operator (better parameterization and controllability) and the Action (more robust and structure-consistent triplet message computation), aligning the evolved program with the needs of reliable graph reasoning.

Listing 1. Iteration 0: Operator `_maybe_lazy_init` and Action `_compute_tri_msgs`

```

1 def _maybe_lazy_init(self, z: _Array, edge_fts: _Array, graph_fts: _Array):
2     in_z = z.shape[-1]
3     in_e = edge_fts.shape[-1]
4     in_g = graph_fts.shape[-1]
5     if self.use_triplets:
6
7         self.t_1 = nn.Linear(in_z, self.nb_triplet_fts)
8         self.t_2 = nn.Linear(in_z, self.nb_triplet_fts)
9         self.t_3 = nn.Linear(in_z, self.nb_triplet_fts)
10        self.t_e_1 = nn.Linear(in_e, self.nb_triplet_fts)
11        self.t_e_2 = nn.Linear(in_e, self.nb_triplet_fts)
12        self.t_e_3 = nn.Linear(in_e, self.nb_triplet_fts)
13        self.t_g = nn.Linear(in_g, self.nb_triplet_fts)
14        self.o3 = nn.Linear(self.nb_triplet_fts, self.out_size)
15
16    def _compute_tri_msgs(
17        self,
18        z: _Array,
19        edge_fts: _Array,
20        graph_fts: _Array,
21    ) -> Optional[_Array]:
22
23
24
25    if not self.use_triplets:
26        return None
27
28
29    tri_1 = self.t_1(z)
30    tri_2 = self.t_2(z)
31    tri_3 = self.t_3(z)
32    tri_e_1 = self.t_e_1(edge_fts)
33    tri_e_2 = self.t_e_2(edge_fts)
34    tri_e_3 = self.t_e_3(edge_fts)
35    tri_g = self.t_g(graph_fts)
36
37    triplets = (
38        tri_1.unsqueeze(2).unsqueeze(3) +
39        tri_2.unsqueeze(1).unsqueeze(3) +
40        tri_3.unsqueeze(1).unsqueeze(2) +
41        tri_e_1.unsqueeze(3) +
42        tri_e_2.unsqueeze(2) +
43        tri_e_3.unsqueeze(1) +
44        tri_g.unsqueeze(1).unsqueeze(2).unsqueeze(3)
45    )
46    tri_msgs = self.o3(torch.amax(triplets, dim=1))
47    if self.activation is not None:
48        tri_msgs = self.activation(tri_msgs)
49
50
51    return tri_msgs

```

Listing 2. Iteration 1: Operator `_maybe_lazy_init` and Action `_compute_tri_msgs`

```

1 def _maybe_lazy_init(self, z: _Array, edge_fts: _Array, graph_fts: _Array):
2     in_z = z.shape[-1]
3     in_e = edge_fts.shape[-1]
4     in_g = graph_fts.shape[-1]
5     if self.use_triplets:
6
7         head_dim = self.nb_triplet_fts // 4
8         self.heads = nn.ModuleList([nn.ModuleDict({
9             't_1': nn.Linear(in_z, head_dim),

```

```

10         't_2': nn.Linear(in_z, head_dim),
11         't_3': nn.Linear(in_z, head_dim),
12         't_e_1': nn.Linear(in_e, head_dim),
13         't_e_2': nn.Linear(in_e, head_dim),
14         't_e_3': nn.Linear(in_e, head_dim),
15         't_g': nn.Linear(in_g, head_dim)
16     }) for _ in range(4)])
17     self.o3 = nn.Linear(4 * head_dim, self.out_size)
18
19     def _compute_tri_msgs(
20         self,
21         z: _Array,
22         edge_fts: _Array,
23         graph_fts: _Array,
24     ) -> Optional[_Array]:
25
26         if not self.use_triplets:
27             return None
28
29
30         head_outputs = []
31         for head in self.heads:
32             tri_1 = head['t_1'](z)
33             tri_2 = head['t_2'](z)
34             tri_3 = head['t_3'](z)
35             tri_e_1 = head['t_e_1'](edge_fts)
36             tri_e_2 = head['t_e_2'](edge_fts)
37             tri_e_3 = head['t_e_3'](edge_fts)
38             tri_g = head['t_g'](graph_fts)
39
40
41             mix_i = tri_1.unsqueeze(2) * tri_2.unsqueeze(1)
42             mix_j = tri_3.unsqueeze(1) * tri_e_2
43             mix_k = tri_e_1 * tri_e_3
44
45
46             head_tri = mix_i + mix_j + mix_k + tri_g.unsqueeze(1).unsqueeze(2)
47             head_outputs.append(head_tri)
48
49
50         triplets = torch.cat(head_outputs, dim=-1)
51         tri_msgs = self.o3(triplets)
52
53         if self.activation is not None:
54             tri_msgs = self.activation(tri_msgs)
55
56
57         return tri_msgs

```

Listing 3. Iteration 2: Operator `_maybe_lazy_init` and Action `_compute_tri_msgs`

```

1 def _maybe_lazy_init(self, z: _Array, edge_fts: _Array, graph_fts: _Array):
2     in_z = z.shape[-1]
3     in_e = edge_fts.shape[-1]
4     in_g = graph_fts.shape[-1]
5     if self.use_triplets:
6
7         half1 = self.nb_triplet_fts // 2
8         half2 = self.nb_triplet_fts - half1
9
10
11         self.t_1_head1 = nn.Linear(in_z, half1)
12         self.t_1_head2 = nn.Linear(in_z, half2)
13         self.t_2_head1 = nn.Linear(in_z, half1)

```

```

14     self.t_2_head2 = nn.Linear(in_z, half2)
15     self.t_3_head1 = nn.Linear(in_z, half1)
16     self.t_3_head2 = nn.Linear(in_z, half2)
17
18
19     self.t_e_1_head1 = nn.Linear(in_e, half1)
20     self.t_e_1_head2 = nn.Linear(in_e, half2)
21     self.t_e_2_head1 = nn.Linear(in_e, half1)
22     self.t_e_2_head2 = nn.Linear(in_e, half2)
23     self.t_e_3_head1 = nn.Linear(in_e, half1)
24     self.t_e_3_head2 = nn.Linear(in_e, half2)
25
26
27     self.t_g_head1 = nn.Linear(in_g, half1)
28     self.t_g_head2 = nn.Linear(in_g, half2)
29
30
31     self.o3 = nn.Linear(self.nb_triplet_fts, self.out_size)
32
33     def _compute_tri_msgs(
34         self,
35         z: _Array,
36         edge_fts: _Array,
37         graph_fts: _Array,
38     ) -> Optional[_Array]:
39
40
41
42     if not self.use_triplets:
43         return None
44
45
46
47     tri_1 = torch.cat([self.t_1_head1(z), self.t_1_head2(z)], dim=-1)
48     tri_2 = torch.cat([self.t_2_head1(z), self.t_2_head2(z)], dim=-1)
49     tri_3 = torch.cat([self.t_3_head1(z), self.t_3_head2(z)], dim=-1)
50     tri_e_1 = torch.cat([self.t_e_1_head1(edge_fts), self.t_e_1_head2(edge_fts)], dim
51 ↪ =-1)
52     tri_e_2 = torch.cat([self.t_e_2_head1(edge_fts), self.t_e_2_head2(edge_fts)], dim
53 ↪ =-1)
54     tri_e_3 = torch.cat([self.t_e_3_head1(edge_fts), self.t_e_3_head2(edge_fts)], dim
55 ↪ =-1)
56     tri_g = torch.cat([self.t_g_head1(graph_fts), self.t_g_head2(graph_fts)], dim=-1)
57
58     triplets = (
59         tri_1.unsqueeze(2).unsqueeze(3) +
60         tri_2.unsqueeze(1).unsqueeze(3) +
61         tri_3.unsqueeze(1).unsqueeze(2) +
62         tri_e_1.unsqueeze(3) +
63         tri_e_2.unsqueeze(2) +
64         tri_e_3.unsqueeze(1) +
65         tri_g.unsqueeze(1).unsqueeze(2).unsqueeze(3)
66     )
67
68     tri_msgs_main = self.o3(torch.amax(triplets, dim=1))
69
70     residual = self.o3(F.relu(tri_e_1))
71     tri_msgs = tri_msgs_main + residual
72
73     if self.activation is not None:
74         tri_msgs = self.activation(tri_msgs)
75

```

```
76 return tri_msgs
```

Listing 4. Iteration 7: Operator `_maybe_lazy_init` and Action `_compute_tri_msgs`

```
1 def _maybe_lazy_init(self, z: _Array, edge_fts: _Array, graph_fts: _Array):
2     in_z = z.shape[-1]
3     in_e = edge_fts.shape[-1]
4     in_g = graph_fts.shape[-1]
5     if self.use_triplets:
6
7         half1 = self.nb_triplet_fts // 2
8         half2 = self.nb_triplet_fts - half1
9
10
11         self.t_1_head1 = nn.Linear(in_z, half1)
12         self.t_1_head2 = nn.Linear(in_z, half2)
13         self.t_2_head1 = nn.Linear(in_z, half1)
14         self.t_2_head2 = nn.Linear(in_z, half2)
15         self.t_3_head1 = nn.Linear(in_z, half1)
16         self.t_3_head2 = nn.Linear(in_z, half2)
17
18
19         self.t_e_1_head1 = nn.Linear(in_e, half1)
20         self.t_e_1_head2 = nn.Linear(in_e, half2)
21         self.t_e_2_head1 = nn.Linear(in_e, half1)
22         self.t_e_2_head2 = nn.Linear(in_e, half2)
23         self.t_e_3_head1 = nn.Linear(in_e, half1)
24         self.t_e_3_head2 = nn.Linear(in_e, half2)
25
26
27         self.t_g_head1 = nn.Linear(in_g, half1)
28         self.t_g_head2 = nn.Linear(in_g, half2)
29
30
31         self.o3 = nn.Linear(self.nb_triplet_fts, self.out_size)
32
33 def _compute_tri_msgs(
34     self,
35     z: _Array,
36     edge_fts: _Array,
37     graph_fts: _Array,
38 ) -> Optional[_Array]:
39
40
41
42     if not self.use_triplets:
43         return None
44
45
46
47     tri_1 = torch.cat([self.t_1_head1(z), self.t_1_head2(z)], dim=-1)
48     tri_2 = torch.cat([self.t_2_head1(z), self.t_2_head2(z)], dim=-1)
49     tri_3 = torch.cat([self.t_3_head1(z), self.t_3_head2(z)], dim=-1)
50     tri_e_1 = torch.cat([self.t_e_1_head1(edge_fts), self.t_e_1_head2(edge_fts)], dim
51     ↪ =-1)
52     tri_e_2 = torch.cat([self.t_e_2_head1(edge_fts), self.t_e_2_head2(edge_fts)], dim
53     ↪ =-1)
54     tri_e_3 = torch.cat([self.t_e_3_head1(edge_fts), self.t_e_3_head2(edge_fts)], dim
55     ↪ =-1)
56     tri_g = torch.cat([self.t_g_head1(graph_fts), self.t_g_head2(graph_fts)], dim=-1)
57
58     triplets = (
59         tri_1.unsqueeze(2).unsqueeze(3) +
60         tri_2.unsqueeze(1).unsqueeze(3) +
61         tri_3.unsqueeze(1).unsqueeze(3) +
62         tri_e_1.unsqueeze(1).unsqueeze(3) +
63         tri_e_2.unsqueeze(1).unsqueeze(3) +
64         tri_e_3.unsqueeze(1).unsqueeze(3) +
65         tri_g.unsqueeze(1).unsqueeze(3)
```

```

58     tri_3.unsqueeze(1).unsqueeze(2) +
59     tri_e_1.unsqueeze(3) +
60     tri_e_2.unsqueeze(2) +
61     tri_e_3.unsqueeze(1) +
62     tri_g.unsqueeze(1).unsqueeze(2).unsqueeze(3)
63 )
64
65
66 tri_msgs_main = self.o3(torch.amax(triplets, dim=1))
67
68
69 residual = self.o3(F.relu(tri_e_1))
70 gate = torch.sigmoid(edge_fts.mean(dim=-1, keepdim=True))
71 residual = residual * gate
72
73 tri_msgs = tri_msgs_main + residual
74
75 if self.activation is not None:
76     tri_msgs = self.activation(tri_msgs)
77
78
79 return tri_msgs

```

Listing 5. Iteration 46: Operator `_maybe_lazy_init` and Action `_compute_tri_msgs`

```

1 def _maybe_lazy_init(self, z: _Array, edge_fts: _Array, graph_fts: _Array):
2     in_z = z.shape[-1]
3     in_e = edge_fts.shape[-1]
4     in_g = graph_fts.shape[-1]
5     if self.use_triplets:
6         quarter = self.nb_triplet_fts // 4
7         quarters = [quarter] * 4
8         quarters[3] = self.nb_triplet_fts - 3 * quarter
9
10    self.t_1_head1 = nn.Linear(in_z, quarters[0])
11    self.t_1_head2 = nn.Linear(in_z, quarters[1])
12    self.t_1_head3 = nn.Linear(in_z, quarters[2])
13    self.t_1_head4 = nn.Linear(in_z, quarters[3])
14    self.t_2_head1 = nn.Linear(in_z, quarters[0])
15    self.t_2_head2 = nn.Linear(in_z, quarters[1])
16    self.t_2_head3 = nn.Linear(in_z, quarters[2])
17    self.t_2_head4 = nn.Linear(in_z, quarters[3])
18    self.t_3_head1 = nn.Linear(in_z, quarters[0])
19    self.t_3_head2 = nn.Linear(in_z, quarters[1])
20    self.t_3_head3 = nn.Linear(in_z, quarters[2])
21    self.t_3_head4 = nn.Linear(in_z, quarters[3])
22
23
24    self.t_e_1_head1 = nn.Linear(in_e, quarters[0])
25    self.t_e_1_head2 = nn.Linear(in_e, quarters[1])
26    self.t_e_1_head3 = nn.Linear(in_e, quarters[2])
27    self.t_e_1_head4 = nn.Linear(in_e, quarters[3])
28    self.t_e_2_head1 = nn.Linear(in_e, quarters[0])
29    self.t_e_2_head2 = nn.Linear(in_e, quarters[1])
30    self.t_e_2_head3 = nn.Linear(in_e, quarters[2])
31    self.t_e_2_head4 = nn.Linear(in_e, quarters[3])
32    self.t_e_3_head1 = nn.Linear(in_e, quarters[0])
33    self.t_e_3_head2 = nn.Linear(in_e, quarters[1])
34    self.t_e_3_head3 = nn.Linear(in_e, quarters[2])
35    self.t_e_3_head4 = nn.Linear(in_e, quarters[3])
36
37
38    self.t_g_head1 = nn.Linear(in_g, quarters[0])
39    self.t_g_head2 = nn.Linear(in_g, quarters[1])

```

```

40     self.t_g_head3 = nn.Linear(in_g, quarters[2])
41     self.t_g_head4 = nn.Linear(in_g, quarters[3])
42
43
44     self.o3 = nn.Linear(self.nb_triplet_fts, self.out_size)
45
46
47     self.aggr_mixer = nn.Linear(2 * self.nb_triplet_fts, self.nb_triplet_fts)
48
49     self.res_gate = nn.Linear(in_e, 1)
50
51 def _compute_tri_msgs(
52     self,
53     z: _Array,
54     edge_fts: _Array,
55     graph_fts: _Array,
56     adj_mat: _Array,
57 ) -> Optional[_Array]:
58
59     if not self.use_triplets:
60         return None
61
62
63
64     tri_1 = torch.cat([
65         self.t_1_head1(z), self.t_1_head2(z),
66         self.t_1_head3(z), self.t_1_head4(z)
67     ], dim=-1)
68     tri_2 = torch.cat([
69         self.t_2_head1(z), self.t_2_head2(z),
70         self.t_2_head3(z), self.t_2_head4(z)
71     ], dim=-1)
72     tri_3 = torch.cat([
73         self.t_3_head1(z), self.t_3_head2(z),
74         self.t_3_head3(z), self.t_3_head4(z)
75     ], dim=-1)
76     tri_e_1 = torch.cat([
77         self.t_e_1_head1(edge_fts), self.t_e_1_head2(edge_fts),
78         self.t_e_1_head3(edge_fts), self.t_e_1_head4(edge_fts)
79     ], dim=-1)
80     tri_e_2 = torch.cat([
81         self.t_e_2_head1(edge_fts), self.t_e_2_head2(edge_fts),
82         self.t_e_2_head3(edge_fts), self.t_e_2_head4(edge_fts)
83     ], dim=-1)
84     tri_e_3 = torch.cat([
85         self.t_e_3_head1(edge_fts), self.t_e_3_head2(edge_fts),
86         self.t_e_3_head3(edge_fts), self.t_e_3_head4(edge_fts)
87     ], dim=-1)
88     tri_g = torch.cat([
89         self.t_g_head1(graph_fts), self.t_g_head2(graph_fts),
90         self.t_g_head3(graph_fts), self.t_g_head4(graph_fts)
91     ], dim=-1)
92
93
94     triplets = (
95         tri_1.unsqueeze(2).unsqueeze(3) +
96         tri_2.unsqueeze(1).unsqueeze(3) +
97         tri_3.unsqueeze(1).unsqueeze(2) +
98         tri_e_1.unsqueeze(3) +
99         tri_e_2.unsqueeze(2) +
100        tri_e_3.unsqueeze(1) +
101        tri_g.unsqueeze(1).unsqueeze(2).unsqueeze(3)
102    )
103
104

```

```

105 max_aggr = torch.amax(triplets, dim=3)
106 mean_aggr = torch.mean(triplets, dim=3)
107 combined = torch.cat([max_aggr, mean_aggr], dim=-1)
108 mixed_aggr = self.aggr_mixer(combined)
109 tri_msgs_main = self.o3(mixed_aggr)
110
111
112 gate = torch.sigmoid(self.res_gate(edge_fts)) * adj_mat.unsqueeze(-1)
113 residual = self.o3(F.relu(tri_e_1)) * gate
114 tri_msgs = tri_msgs_main + residual
115
116
117 tri_msgs = tri_msgs * adj_mat.unsqueeze(-1)
118
119 if self.activation is not None:
120     tri_msgs = self.activation(tri_msgs)
121
122
123 return tri_msgs

```

Listing 6. Iteration 57: Operator `_maybe_lazy_init` and Action `_compute_triplets`

```

1 def _maybe_lazy_init(self, z: _Array, edge_fts: _Array, graph_fts: _Array):
2     in_z = z.shape[-1]
3     in_e = edge_fts.shape[-1]
4     in_g = graph_fts.shape[-1]
5     if self.use_triplets:
6
7         half1 = self.nb_triplet_fts // 2
8         half2 = self.nb_triplet_fts - half1
9
10
11         self.t_1_head1 = nn.Linear(in_z, half1)
12         self.t_1_head2 = nn.Linear(in_z, half2)
13         self.t_2_head1 = nn.Linear(in_z, half1)
14         self.t_2_head2 = nn.Linear(in_z, half2)
15         self.t_3_head1 = nn.Linear(in_z, half1)
16         self.t_3_head2 = nn.Linear(in_z, half2)
17
18
19         self.t_e_1_head1 = nn.Linear(in_e, half1)
20         self.t_e_1_head2 = nn.Linear(in_e, half2)
21         self.t_e_2_head1 = nn.Linear(in_e, half1)
22         self.t_e_2_head2 = nn.Linear(in_e, half2)
23         self.t_e_3_head1 = nn.Linear(in_e, half1)
24         self.t_e_3_head2 = nn.Linear(in_e, half2)
25
26
27         self.t_g_head1 = nn.Linear(in_g, half1)
28         self.t_g_head2 = nn.Linear(in_g, half2)
29
30
31         self.o3 = nn.Linear(self.nb_triplet_fts, self.out_size)
32
33
34         self.aggr_mixer = nn.Linear(2 * self.nb_triplet_fts, self.nb_triplet_fts)
35         self.res_gate = nn.Linear(in_e + in_g, 1)
36
37
38         self.gate_node = nn.Linear(in_z, 6)
39         self.gate_edge = nn.Linear(in_e, 6)
40         self.gate_global = nn.Linear(in_g, 2)
41
42 def _compute_triplets(

```

```

43     self,
44     z: _Array,
45     edge_fts: _Array,
46     graph_fts: _Array,
47 ) -> Optional[_Array]:
48
49
50
51 if not self.use_triplets:
52     return None
53
54
55
56 gate_node_all = torch.sigmoid(self.gate_node(z))
57 gate_edge_all = torch.sigmoid(self.gate_edge(edge_fts))
58 gate_global = torch.sigmoid(self.gate_global(graph_fts))
59
60
61
62 gate_t1 = gate_node_all[..., 0:2]
63 gate_t2 = gate_node_all[..., 2:4]
64 gate_t3 = gate_node_all[..., 4:6]
65
66 tri_1 = torch.cat([
67     self.t_1_head1(z) * gate_t1[..., 0:1],
68     self.t_1_head2(z) * gate_t1[..., 1:2]
69 ], dim=-1)
70 tri_2 = torch.cat([
71     self.t_2_head1(z) * gate_t2[..., 0:1],
72     self.t_2_head2(z) * gate_t2[..., 1:2]
73 ], dim=-1)
74 tri_3 = torch.cat([
75     self.t_3_head1(z) * gate_t3[..., 0:1],
76     self.t_3_head2(z) * gate_t3[..., 1:2]
77 ], dim=-1)
78
79
80 gate_te1 = gate_edge_all[..., 0:2]
81 gate_te2 = gate_edge_all[..., 2:4]
82 gate_te3 = gate_edge_all[..., 4:6]
83
84 tri_e_1 = torch.cat([
85     self.t_e_1_head1(edge_fts) * gate_te1[..., 0:1],
86     self.t_e_1_head2(edge_fts) * gate_te1[..., 1:2]
87 ], dim=-1)
88 tri_e_2 = torch.cat([
89     self.t_e_2_head1(edge_fts) * gate_te2[..., 0:1],
90     self.t_e_2_head2(edge_fts) * gate_te2[..., 1:2]
91 ], dim=-1)
92 tri_e_3 = torch.cat([
93     self.t_e_3_head1(edge_fts) * gate_te3[..., 0:1],
94     self.t_e_3_head2(edge_fts) * gate_te3[..., 1:2]
95 ], dim=-1)
96
97
98 tri_g = torch.cat([
99     self.t_g_head1(graph_fts) * gate_global[:, 0:1],
100    self.t_g_head2(graph_fts) * gate_global[:, 1:2]
101 ], dim=-1)
102
103 triplets = (
104     tri_1.unsqueeze(2).unsqueeze(3) +
105     tri_2.unsqueeze(1).unsqueeze(3) +
106     tri_3.unsqueeze(1).unsqueeze(2) +
107     tri_e_1.unsqueeze(3) +

```

```
108     tri_e_2.unsqueeze(2) +
109     tri_e_3.unsqueeze(1) +
110     tri_g.unsqueeze(1).unsqueeze(2).unsqueeze(3)
111 )
112
113
114 max_aggr = torch.amax(triplets, dim=3)
115 mean_aggr = torch.mean(triplets, dim=3)
116 combined = torch.cat([max_aggr, mean_aggr], dim=-1)
117 mixed_aggr = self.aggr_mixer(combined)
118 tri_msgs_main = self.o3(mixed_aggr)
119
120
121 graph_fts_expanded = graph_fts.unsqueeze(1).unsqueeze(2).expand(
122     -1, edge_fts.shape[1], edge_fts.shape[2], -1)
123 gate_input = torch.cat([edge_fts, graph_fts_expanded], dim=-1)
124 gate = torch.sigmoid(self.res_gate(gate_input))
125 residual = self.o3(F.relu(tri_e_1)) * gate
126 tri_msgs = tri_msgs_main + residual
127
128 if self.activation is not None:
129     tri_msgs = self.activation(tri_msgs)
130
131
132 return tri_msgs
```